

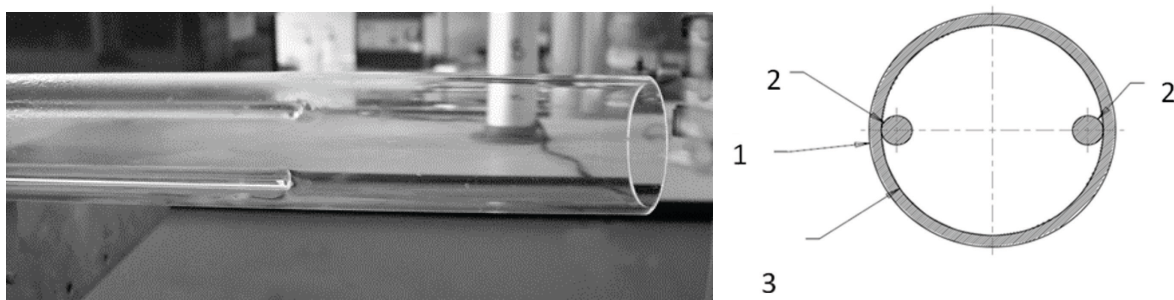
Supporting information

1. Results and Discussion

1.1. Design and Modification of a Rotary Furnace

The quartz tube modification is shown in Figure S1. Two small quartz rod blades of $\text{Ø}5$ mm were oppositely attached to quartz tube.

Figure S1. Image (left) and sketch (right) of a new tube with baffles inside, created by adding two quartz rods inside the normal quartz tube.



In order to move the batch process to a continuous production, a continuous feeding system was designed using a 20 mL syringe piston feeder which was connected to a push type 'T' junction, as shown in Figure S2.

Figure S2. Sketch (a) and picture (b) of a new gas blow feeding system, to realise continuous feeding.

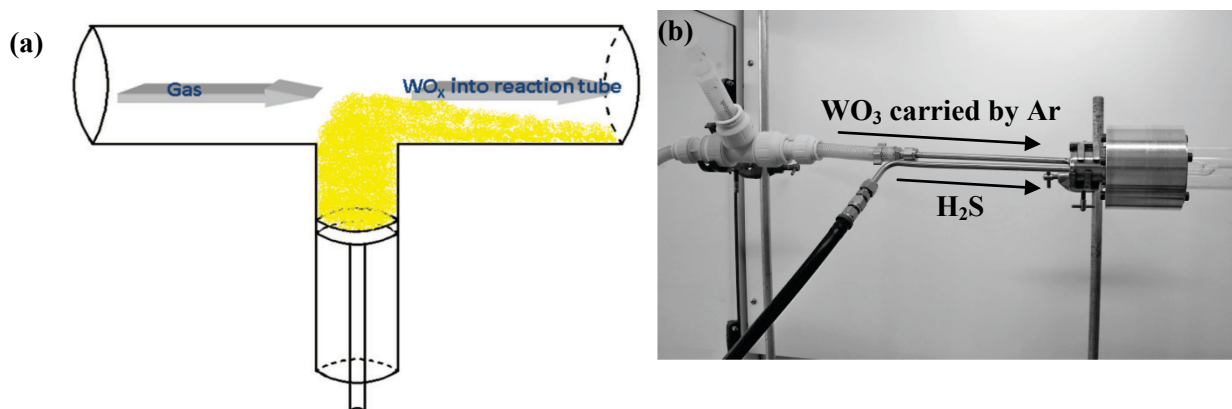
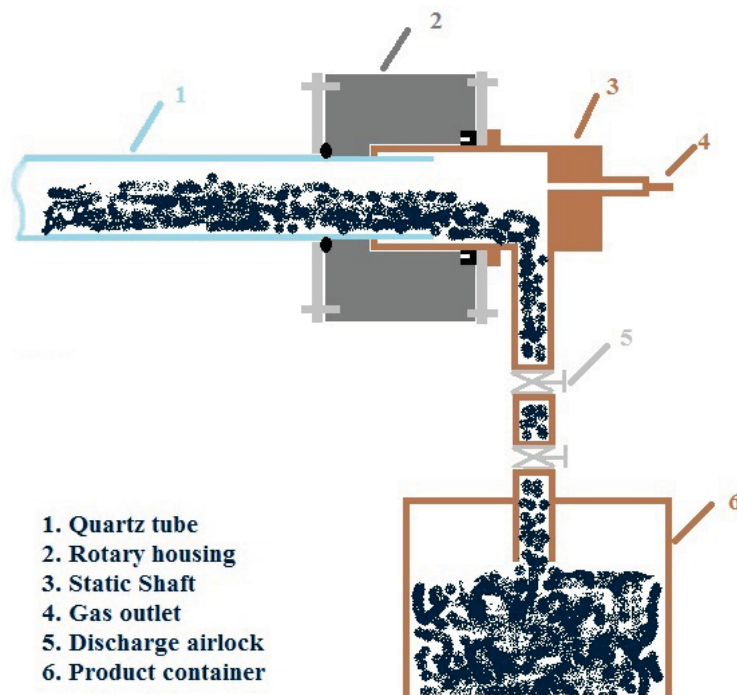


Figure S3. Sketch of the collection system, where (1) quartz tube and (2) housing are rotating while all other parts are kept still during action.



The collection system makes the process a real continuous one, as shown in Figure S3. During the process, the quartz tube (1) and housing were driven to rotate by the motor, while the shaft (3) was kept static, as well as the gas outlet (4) and collection outlet (5 and 6) attached to it. Note that the product discharge outlet allows for easy isolation to collect samples for quality control during the manufacturing.

2.2. *IF-WS₂ Synthesis by Different Methods*

2.2.1. Mixed WO₃ and S with H₂

The SEM images of the as-received WO₃ precursor have been displayed in Figure S4; and the average particles size was about 60 nm, estimated using Derby-Scherrer Equation. The XRD pattern shown in Figure S5 matches very well with the monoclinic WO₃ (JCPDS No. 43-1035).

Figure S4. SEM images of the as-received WO₃ nanoparticles (~60 nm in size).

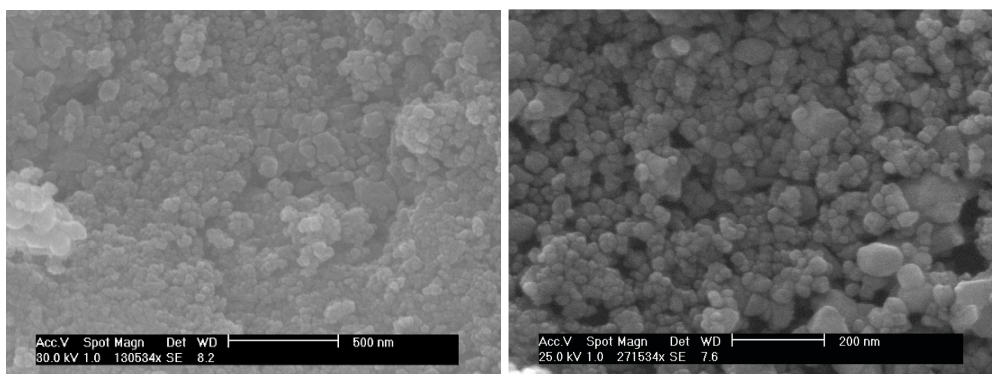
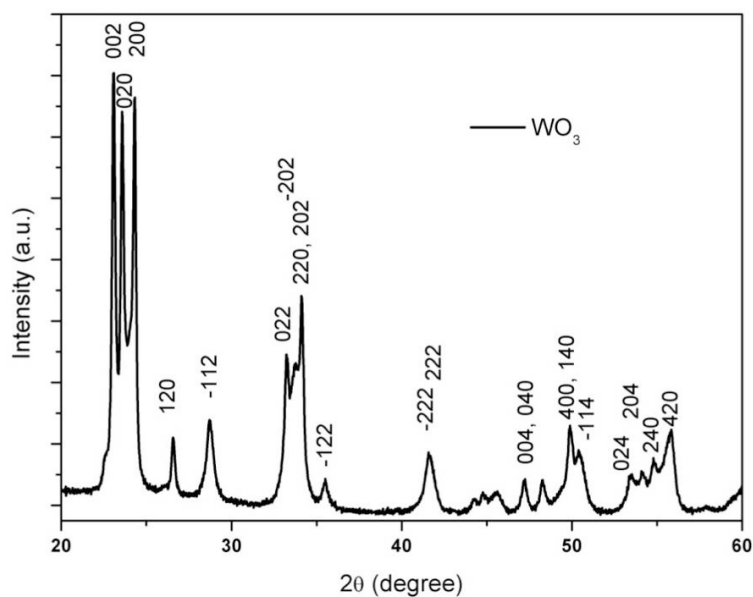


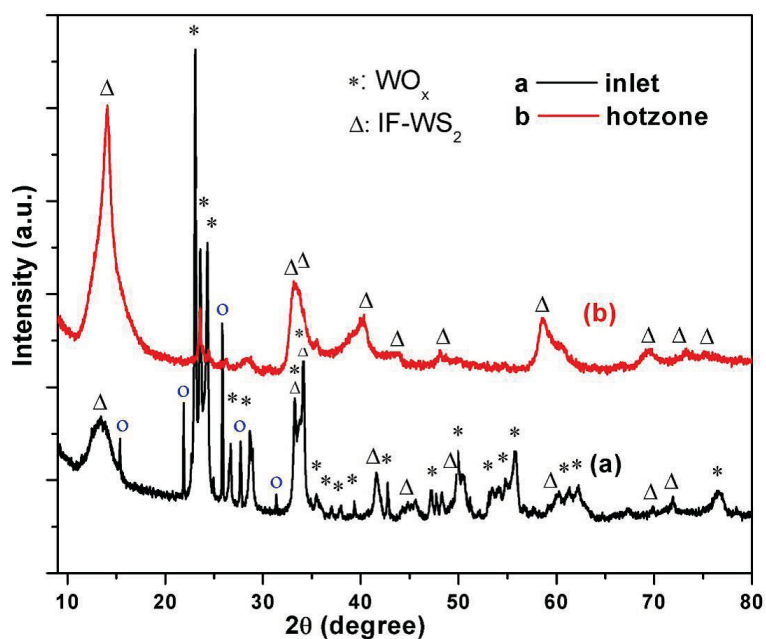
Figure S5. XRD pattern of the as-received WO_3 precursor.



2.2.1. WO_3 and S reaction under H_2

The XRD patterns of Sample S2 from both the inlet and the hot zones are shown in Figure S6. Only a few WS_2 layers may have formed, as the majority was WO_x , along with S peaks (labelled with circle), although the hot zone samples exhibited a more complete oxide-to-sulphide conversion.

Figure S6. XRD patterns of Sample S2. (a) from the inlet zone and (b) from the central hot zone.



2.2.2. APT as Precursor and H₂S as Reaction Gas—Production of WO_x Nanoparticles from APT

WO_x nanoparticles, as an important precursor for IF-WS₂ nanoparticles, have been produced by the decomposition of APT at a high temperature furnace. At high temperature, the following reaction took place: $(\text{NH}_4)_{10}[\text{H}_2\text{W}_{12}\text{O}_{42}] \cdot 4\text{H}_2\text{O} \rightarrow 12 \text{WO}_3 + 10\text{NH}_3 + 11\text{H}_2\text{O}$.

In fact, the APT started to decompose into WO₃ at 500 °C. The WO₃ then started to melt and vaporise in the central zone where temperature reached 1200 °C and 1250 °C respectively, and the WO_x vapour would be brought downstream by the Ar flow and deposit at the inner wall of the quartz tube.

After optimization of the parameters, very fine nanoparticles with high batch yield were produced at 1350 °C, with long quartz tube (1.5 m) and high gas flow rate (6 L/min). The results were shown in Figure S7a–c. Both spherical and polyhedral particles are presented in all images, with uniform size less than 100 nm, mostly around 50 nm. XRD pattern in Figure S7d matches very well with monoclinic WO₃ (JCPDS No. 43-1035), with the strongest peaks appear at 23–25 degree.

Figure S7. SEM images (a–c), and XRD pattern (d) of tungsten oxide nanoparticle (1350°C, 6 L/min, 30 min, 1.5 m).

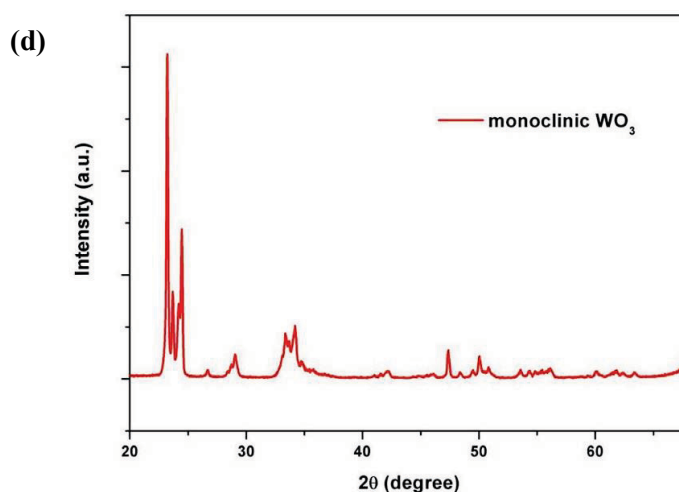


Figure S8. TEM images of WO₃ from decomposition of APT (1350, 1.5 m, 6 L/min, 30 min).

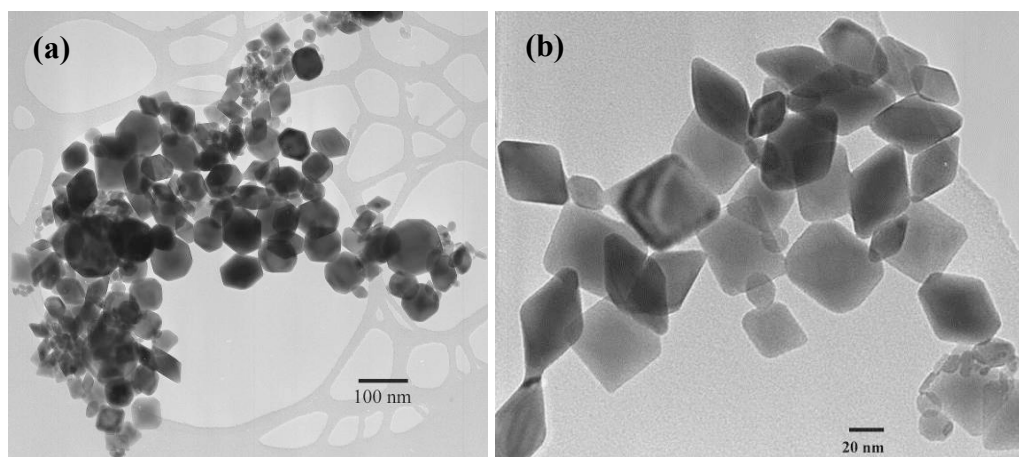
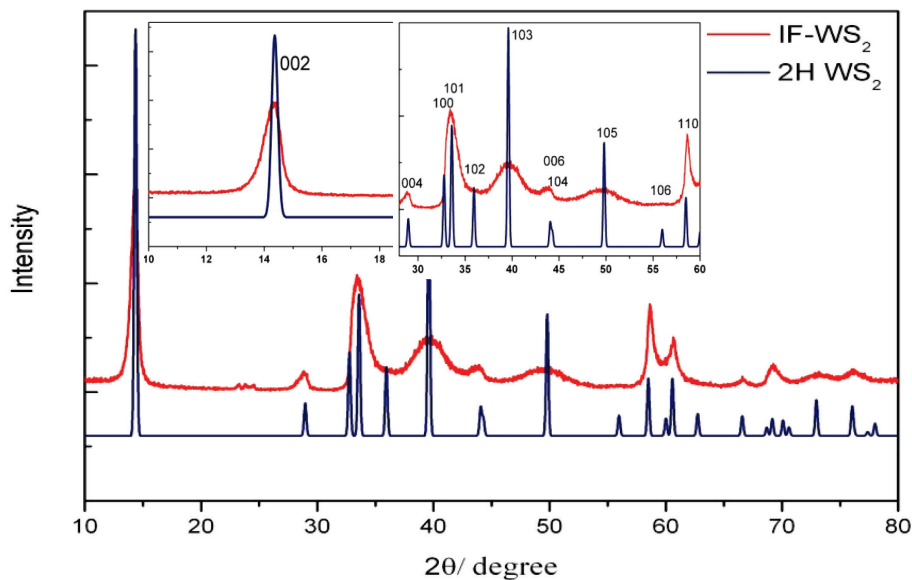


Figure S8 shows the TEM images of WO_3 nanoparticles from the decomposition of APT. The majority of nanoparticles are of a polyhedral shape, around 50 nm.

2.2.3. WO_3 and H_2S Synthesis of WS_2 Nanomaterials

Figure S9. XRD profiles of commercial 2H- WS_2 and currently synthesised IF- WS_2 .



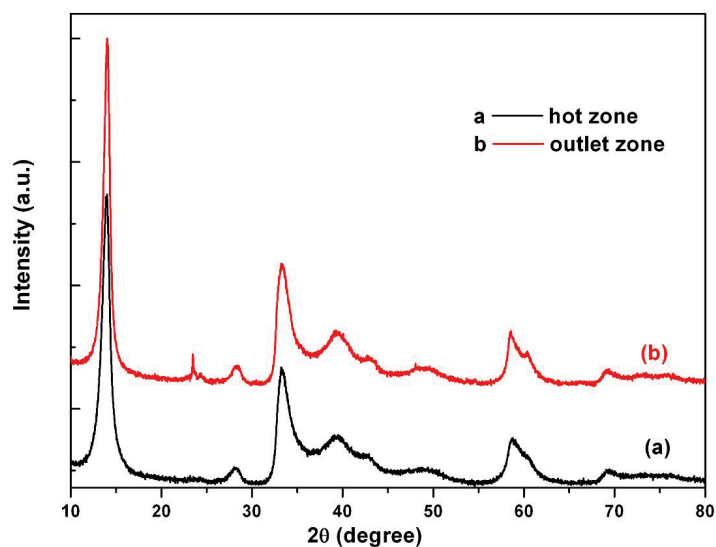
A comparison of the XRD profiles of the commercial 2H- WS_2 and the present IF- WS_2 samples is shown in Figure S9. Both patterns showed peaks at very similar positions. The peaks of IF- WS_2 were assigned according to 2H- WS_2 (JCPDS No. 84-1398), as no standard XRD pattern is available for IF- WS_2 [1]. These are the typical peaks at 2θ angles at: 14.364 (002), 28.959 (004), 32.769 (100), 33.587 (101), 35.943 (102), 39.599 (103), 44.055 (006), 44.289 (104), 49.798 (105), 55.977 (106), 57.495 (110), 60.010 (008), 60.573 (112), 62.746 (107), 69.169 (201), 70.080 (108), 72.957(203), and 76.040(116). For the 2H- WS_2 , all peaks are very sharp, indicating a well-crystallized and standard 2H structure. Its (002) is the strongest peak, followed by (103) as the second strongest. Compared with 2H- WS_2 , the (002) peak of IF- WS_2 is left-shifted, indicating a lattice expansion of the (002) layers due to stains in the curved closed-cage layers [2]. The (103) and (105) peaks are broadened, attributing to the ultra-low dimensions. Whilst the (002) remains as the strongest peak, two peaks representing (100) and (101) have merged into one exhibiting the second highest intensity. The (006) and (104) peaks also merged, at around 44.1 degree. The (102) peak at around 35.9 degree was not detected in the IF- WS_2 profile. The small peaks appeared at 23-25 degree in the IF- WS_2 pattern were assigned to WO_x , which must exist as the residue core of some IF- WS_2 particles.

2.3. Further Refinement and Modification

2.3.1. IF-WS₂ Synthesis Using a Continuous Feeding System—Experiments Based on Both New Feeding System and Baffled Tubes are Named FB_n

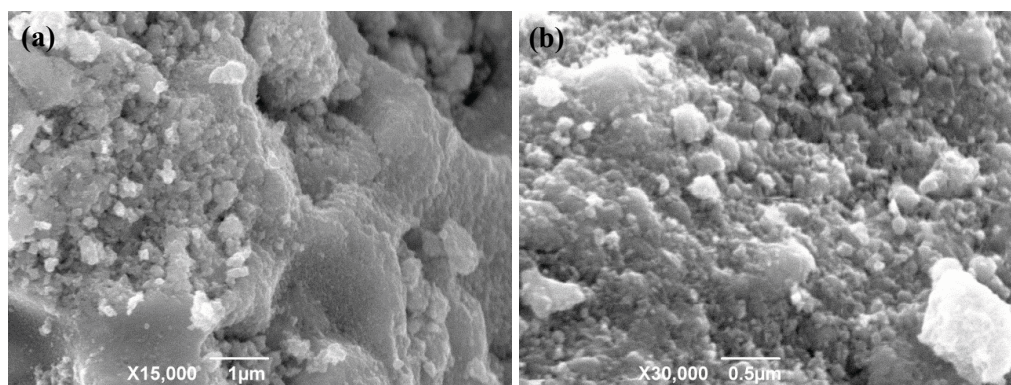
The XRD patterns of samples collected from Sample FB1 (Figure S10) demonstrate a completely conversion of WO_x into WS₂. No WO_x peaks for the hot zone samples and extremely minor peaks of WO_x for the outlet zone samples.

Figure S10. XRD profiles of samples collected from different reaction zones in experiment FB1.



The SEM images in Figure S11 have revealed the morphology of particles collected from the hot zone in FB1. The particles were quite uniform, with sizes no more than 100 nm. The very bright pieces at the right bottom corner of Figure S11b could be residue S, owing to the excessive amount of H₂S gas used.

Figure S11. SEM images for particles collected from hot zone of experiment FB1.



References

1. Feldman, Y.; Frey, G.L.; Homyonfer, M.; Lyakhovitskaya, V.; Margulis, L.; Cohen, H.; Hodes, G.; Hutchison, J.L.; Tenne, R. Bulk synthesis of inorganic fullerene-like MS_2 ($M = Mo, W$) from the respective trioxides and the reaction mechanism. *J. Am. Chem. Soc.* **1996**, *118*, 5362–5367.
2. Feldman, Y.; Wasserman, E.; Srolovitz, D.J.; Tenne, R. High rate, gas phase growth of MoS_2 nested inorganic fullerenes and nanotubes. *Science* **1995**, *267*, 222–225.

© 2014 by the authors; licensee MDPI, Basel, Switzerland. This article is an open access article distributed under the terms and conditions of the Creative Commons Attribution license (<http://creativecommons.org/licenses/by/3.0/>).